narra j

Short Communication

Mesenchymal stem cell-derived secretome accelerates third-degree burn wound healing: Effects on proliferation, angiogenesis, and fibrosis regulation

Bayu T. Dirja[1*], Agung Putra[2,3] and Nur D. Amalina[3,4]

[1]Faculty of Medicine, Universitas Mataram, Lombok, Indonesia; [2]Department of Pathology Anatomy, Faculty of Medicine, Universitas Islam Sultan Agung, Semarang, Indonesia; [3]Stem Cell and Cancer Research Indonesia, Semarang, Indonesia; [4]Department of Pharmaceutical Sciences, Faculty of Medicine, Universitas Negeri Semarang, Semarang, Indonesia

*Corresponding author: bayutirtadirja@gmail.com

Abstract

Mesenchymal stem cell-derived secretome (MSC-derived secretome) has shown promise in regenerative medicine; however, research specifically evaluating its efficacy in third-degree burn wounds remains scarce. The aim of this study was to investigate the effects of MSC-derived secretome on cellular proliferation, angiogenesis, myofibroblast activity, and collagen synthesis in a third-degree burn wound model. A total of 20 Wistar rats were randomly assigned to four groups: a healthy control group, a negative control group with untreated third-degree burn wounds, and two treatment groups receiving MSC-derived secretome at doses of 100 µL and 200 µL for 14 days. The wound healing was assessed 14 days post-treatment. Proliferating cell nuclear antigen (PCNA) protein expression was quantified via Western blot to assess cell proliferation; *vascular endothelial growth factor* (*VEGF*) gene expression was analyzed using quantitative reverse transcription polymerase chain reaction (qRT-PCR) to examine angiogenesis; alpha-smooth muscle actin (α-SMA) expression was assessed through immunohistochemistry to evaluate myofibroblast activity; and collagen density was measured using Masson's trichrome staining to determine tissue remodeling. Our data indicated that MSC-derived secretome treatment significantly enhanced multiple aspects of the healing process in a dose-dependent manner. PCNA expression increased by 2.8-fold in the 200 µL MSC-derived secretome group compared to the negative control ($p<0.05$). *VEGF* gene expression was upregulated by 2.14-fold in the 200 µL secretome group compared to the negative control ($p<0.05$). α-SMA protein expression increased by 12.67% in the 200 µL secretome group, while collagen density demonstrated the most pronounced improvement at the 200 µL dose, reaching an increase of 81.26% ($p<0.05$). In conclusion, MSC-derived secretome significantly accelerates burn wound healing by promoting cell proliferation, enhancing angiogenesis, and increasing collagen synthesis while modulating myofibroblast activity. This highlights the potential of MSC-derived secretome as a therapeutic option for optimizing burn wound repair and reducing fibrotic complications.

Keywords: Burn wound, secretome, proliferation, angiogenesis, fibrosis

Introduction

Third-degree burn wound presents significant clinical challenges due to their depth and severity, often resulting in extensive tissue damage and prolonged healing [1]. It also contributes to substantial morbidity, including infections and scarring, and is associated with high mortality

https://narraj.org/

Received: November 30, 2024 - Accepted: March 26, 2025 - Published online: May 19, 2025

rates [2]. Despite advances in burn care, third-degree burn remains a major global health concern, accounting for approximately 180,000 deaths annually and leaving millions with burn-related disabilities, highlighting the urgent need for improved therapeutic strategies [3].

Comprehensive clinical management protocols have been established to address the severity of burn injuries, including autologous skin grafting [4]. However, autologous grafts have limitations that affect their effectiveness and patient outcomes, such as donor site morbidity, limited availability, graft failure, and infection risk [5,6]. These challenges pose a significant barrier to optimal burn management, particularly in patients with extensive burns where donor sites are scarce. Additionally, conventional treatments often lead to hypertrophic scarring and contractures, which contribute to functional impairment and psychological distress, reinforcing the need for alternative therapeutic approaches [7].

Effective burn wound repair is essential for restoring tissue integrity and function, as any disruption in this process can result in impaired healing or chronic, non-healing wounds [1]. Burn wound repair is regulated by key molecular mediators, including the cell cycle regulator proliferating cell nuclear antigen (PCNA), which governs cellular proliferation; vascular endothelial growth factor (VEGF), which promotes neovascularization; and collagen, which is crucial for extracellular matrix reconstruction and remodeling [8,9]. PCNA functions as a critical cofactor that enhances DNA polymerase processivity, thereby facilitating cellular division and tissue repair at burn-injured sites [10]. Increased PCNA expression indicates enhanced cell proliferation, which is essential for re-epithelialization and granulation tissue formation. VEGF plays a central role in angiogenesis by stimulating endothelial cell migration and proliferation, leading to the formation of new capillary networks [11,12]. Adequate angiogenesis is crucial for oxygen and nutrient delivery to the healing wound, while VEGF also promotes re-epithelialization and collagen deposition [13]. Although various therapeutic agents have been explored to enhance burn wound healing, most target isolated aspects of the repair process, limiting their overall efficacy. Given the complexity of burn wound healing, a comprehensive therapeutic approach that simultaneously addresses multiple mechanisms is essential [14].

Recent advances in regenerative medicine suggest that mesenchymal stem cell-derived secretome (MSC-derived secretome) offers significant promise as an innovative intervention for enhancing burn wound repair [15,16]. Unlike conventional treatments or cellular therapies, MSC-derived secretome provides a cell-free approach with several advantages, including reduced immunogenicity, improved storage and handling, greater standardization potential, and the absence of risks associated with tumorigenicity or aberrant differentiation [15-17]. MSC-derived secretome contains a diverse array of bioactive molecules, including growth factors and immunomodulatory cytokines [18], which play critical roles in regulating inflammation, promoting neovascularization, and enhancing tissue regeneration [19-22]. Key signaling molecules such as interleukin-10 (IL-10), transforming growth factor beta (TGF-β), and VEGF are essential mediators of wound repair processes [23,24]. A previous study indicated that MSC-derived secretome enhanced burn wound healing by stimulating dermal fibroblast activity and increasing vascular density, thereby accelerating tissue revascularization [25]. Other studies have demonstrated that mesenchymal stem cells (MSCs) accelerated burn wound healing by inducing angiogenesis through VEGF stimulation, preventing scar formation, and promoting normal skin function [26,27]. VEGF and other growth factors also contribute to the proliferative phase of burn wound healing by inhibiting apoptosis in burn wound models [13]. Additionally, MSC-derived secretome regulate extracellular matrix formation and collagen deposition via the TGF-β pathway, thereby reducing inflammation and minimizing hypertrophic scar formation following burns [28]. Increased TGF-β expression has been associated with smooth muscle actin (α-SMA) production in burn patients, contributing to collagen synthesis [29].

Despite these promising findings, the comprehensive effects of MSC-derived secretome on third-degree burn healing remain insufficiently understood. Given that third-degree burns represent the most severe and challenging category, a deeper investigation into the integrated effects of MSC-derived secretome on proliferation, angiogenesis, and fibrosis regulation is essential. Therefore, the aim of this study was to investigate the effect of MSC-derived secretome on third-degree burn wound closure, with a specific focus on cellular proliferation, angiogenesis, and fibrosis regulation—key processes that, when properly modulated, could significantly

enhance healing outcomes and reduce complications associated with severe burns. This approach is expected to address the critical need for therapies that simultaneously target multiple healing mechanisms, potentially providing a more effective alternative to current burn management strategies, which often require multiple interventions with limited success.

Methods

Study design and setting

An in vivo study was conducted at the Animal Research Laboratory, Stem Cell and Cancer Research, Semarang, Indonesia, using a controlled experimental design to evaluate burn wound healing. The experimental setting was a climate-controlled vivarium maintaining a consistent temperature and humidity, with a 12-hour light/dark cycle. The animal model, male Wistar rats, was maintained for a total duration of 21 days, including a 7-day acclimatization period under standardized laboratory conditions.

On the first day of the experiment, the third-degree burn wound was made on the dorsal area of each rat using hot metal plate. Immediately following burn induction, rats were randomly assigned to treatment groups receiving intradermal MSC-derived secretome at two different volumes (100 µL and 200 µL) or 0.9% NaCl. Wound healing progression was monitored over a 14-day post-treatment period. On day 14, rats were terminally anesthetized for comprehensive wound analysis. The study evaluated key regenerative markers, including *VEGF* gene expression (measured by qRT-PCR), PCNA protein expression (analyzed via Western blot), α-SMA expression (determined by immunohistochemistry), and collagen deposition (assessed using Masson's trichrome staining).

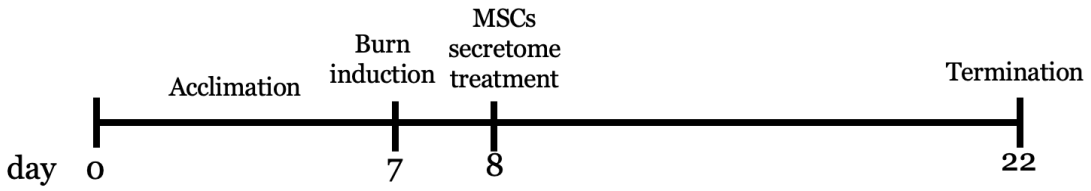

Figure 1. Schematic outline of the study design for evaluating mesenchymal stem cell-derived secretome in third-degree burn wound healing.

Sample size, randomization, blinding, and study group allocation

The sample size was determined using Federer's formula, with a minimum of five rats per group. The total sample size was adjusted to account for possible dropouts, ensuring adequate statistical power throughout the study. Following a 7-day acclimatization period, the animals were randomly allocated into four groups: a healthy group, a negative control group (third-degree burn receiving NaCl treatment), and two experimental groups receiving intradermal administration of MSC-derived secretome at doses of 100 µL and 200 µL. Randomization was conducted using a computer-generated sequence, with rats assigned to treatment groups through a block randomization method. To maintain blinding, animal identification was coded, ensuring that researchers responsible for wound assessment and molecular analyses remained unaware of group assignments. A single investigator retained the randomization key to preserve research integrity.

Animal model

Adult male Wistar rats (*Rattus Novergicus*) aged 8–10 weeks, weighing 200–250 grams and free from pre-existing health conditions, were included in this study. Rats with visible skin abnormalities, signs of infection, or significant weight variations exceeding ±10% of their initial weight were excluded. Dropout criteria included severe distress, weight loss exceeding 15%, signs of infection, or inability to complete the full 22-day experimental protocol. Animal health, wound progression, and potential dropout indicators were monitored daily through weight measurements, wound documentation, and behavioral observations. In cases of potential

dropout, a veterinary expert conducted an immediate assessment of animals showing significant health deterioration.

Animal preparation

The animals were housed under strictly controlled laboratory conditions at the Animal Facility of Stem Cells and Cancer Research, Semarang, Indonesia. Prior to the study, the rats underwent a 7-day acclimatization period to standardize physiological parameters and minimize stress. The rats were housed in polycarbonate cages under controlled environmental conditions, with temperature maintained at 22±2°C, relative humidity at 50–60%, and a 12-hour light-dark cycle (light phase from 06:00 to 18:00). Nutritional management included *ad libitum* access to a standardized rodent pellet diet (protein content: 20–22%, sourced from a certified manufacturer) and sterile filtered water. Cage bedding consisted of sterile wood shavings, replaced twice weekly to maintain hygiene. Each cage housed 4–5 rats to prevent social isolation while avoiding overcrowding. Environmental parameters, including temperature, humidity, and light exposure, were monitored daily to ensure consistency. Animal health assessments were performed regularly through clinical observations, including weight monitoring, activity levels, and physical examination.

Mesenchymal stem cell isolation

MSCs were isolated from rat umbilical cords at gestational day 19 following established protocols with modifications [30]. Briefly, umbilical cord tissue was carefully extracted under sterile conditions and processed for cell culture. The isolated tissue was enzymatically digested and cultured in Dulbecco's Modified Eagle Medium (DMEM) supplemented with 10% fetal bovine serum (FBS) and penicillin/streptomycin (100 IU/mL) to support cell growth and maintain sterility. Cultures were maintained under normoxic conditions at 37°C with 5% CO_2 to ensure optimal proliferation and viability. Cells were routinely monitored, and passages were conducted upon reaching 80% confluence. For experimental procedures, the fifth passage of MSCs was utilized to ensure consistency in cellular characteristics and functional properties.

Mesenchymal stem cell validation and characterization

MSC characterization was performed on the fourth passage of MSCs using a BD Accuri C6 PLUS flow cytometry (BD Biosciences, San Jose, CA, USA) following immunostaining with specific antibodies: APC-CD73, FITC-CD90, PerCP-CD105, and PE-conjugated Lin markers (all from BD Biosciences, San Jose, CA, USA). Cells were incubated with antibodies for 30 minutes at 4°C. Unstained cells and isotype controls were included to ensure specificity in marker expression analysis. Multipotency was evaluated through osteogenic and adipogenic differentiation assays. For osteogenic differentiation, MSCs (4×10^4 cells) were cultured in high-glucose DMEM supplemented with 10% FBS, 1% penicillin-streptomycin, sodium β-glycerophosphate (1×10^{-2} M), dexamethasone (1×10^{-4} M), and ascorbic acid (5×10^{-5} M) for 15 days. The medium was replaced every three days to maintain optimal differentiation conditions. Calcium deposition, indicative of osteogenic differentiation, was visualized using Alizarin Red staining. For adipogenic differentiation, MSCs were cultured in adipogenic medium containing dexamethasone (0.5 µM), isobutyl methylxanthine (0.5 mM), and indomethacin (50 µM) for 21 days. Lipid droplet formation was confirmed using Oil Red O staining. Control cells were maintained in basal medium throughout the study to distinguish spontaneous differentiation from induced differentiation [21,31-33].

Mesenchymal stem cell-derived secretome preparation

MSCs were maintained under hypoxic conditions (5% O_2, 5% CO_2, balanced N_2) at 37°C for 24 hours in a serum-free medium. Following incubation, the conditioned medium was collected and subjected to centrifugation at 2000 rpm for 20 minutes at 8°C to remove cellular debris. The supernatant was then filtered through a 0.22 µm membrane to ensure sterility and purity. Molecules within the 10–50 kDa range were selectively isolated using tangential flow filtration, targeting bioactive factors such as IL-10 (18 kDa) and TGF-β (25 kDa) [34]. The processed hypoxia-preconditioned MSCs were stored at 2–8°C until further use to maintain biological stability [34,35].

Third-degree burn wound induction

Anesthesia was administered via intramuscular injection using a 100 mL cocktail containing ketamine (50 mg/kg), xylazine (10 mg/kg), and acepromazine (2 mg/kg). The dorsal surface was shaved and disinfected with povidone-iodine followed by ethanol. Burn injuries were induced by applying a 1×1 cm metal object, heated to 80°C and weighing 1000 grams, to the skin for 10 seconds. The wounds were left uncovered to allow air exposure. Two animals from the experimental group were excluded due to excessive bleeding during burn wound induction, which compromised wound integrity and resulted in non-representative healing.

Administration of mesenchymal stem cell-derived secretome

On the first day following burn injury, hypoxic MSC-derived secretome was administered intradermally once daily at four distinct sites surrounding the wound margin. The MSC-derived secretome was administered in two dose volumes (100 µL and 200 µL), while the negative control group received an equivalent volume of saline via the same route and schedule. Rats displaying signs of illness, infection, or abnormal behavior during the experiment were excluded. Additionally, animals that experienced excessive bleeding or other complications during burn wound induction were removed from the study.

Skin tissue harvesting

Fourteen days after burn induction, skin tissue was collected for analysis. The excised samples included the burn wound site and surrounding tissue, which were processed for histological and molecular evaluations. The harvested tissue was divided into two portions: one was stored in an RNAase-free cryotube at -80°C for gene expression analysis, while the other was preserved in liquid nitrogen for protein analysis. Collagen deposition was assessed using Masson's trichrome staining [36,37].

VEGF gene expression

Total RNA was extracted from healed skin tissue using Trizol (Invitrogen, Waltham, USA) following the manufacturer's protocol. First-strand complementary DNA (cDNA) synthesis was performed using 1 µg of total RNA and SuperScript II (Invitrogen, Waltham, USA). Reverse transcription-quantitative polymerase chain reaction (RT-qPCR) was conducted with SYBR Green I dye (Invitrogen, Waltham, USA) on an ABI 7500 fluorescence quantitative PCR system (Applied Biosystems, Waltham, USA) to assess the mRNA expression levels of *VEGF* and *B-actin* using specific primers (**Table 1**). The thermocycling protocol included an initial denaturation at 95°C for 10 minutes, followed by 50 cycles of denaturation at 95°C for 15 seconds and annealing/extension at 60°C for one minute. Expression levels were quantified using cycle threshold (Ct) values, and data analysis was performed with the 7500 Software (Applied Biosystems Life Technologies, Foster City, CA, USA) using the 2−ΔΔCt method. All reactions were conducted in triplicate to ensure reproducibility.

Table 1. Primer sequences used for quantitative reverse transcription polymerase chain reaction (qRT-PCR) to identify *VEGF* gene expression in mice

Gene	Primer sequence
Vascular endothelial growth factor (VEGF)	Forward 5'-CTGCTGTAACGATGAAGCCCTG-3' Reverse 5'-GCTGTAGGAAGCTCATCTCTCC-3'
B-actin	Forward 5'- TGCTGTCCCTGTATGCCTCTG-3' Reverse 5'- TGATGTCACGCACGATTTCC-3'

PCNA protein expression

Tissue proteins were extracted using radioimmunoprecipitation assay (RIPA) buffer (Sigma-Aldrich, St. Louis, USA) and quantified with the Pierce bicinchoninic acid (BCA) protein assay. Protein samples (10 µg) were mixed with Laemmli buffer at a 1:1 ratio (Bio-Rad, Hercules, USA), denatured, and resolved on a 10% sodium dodecyl sulfate-polyacrylamide gel electrophoresis (SDS-PAGE) (Bio-Rad, Hercules, USA). Proteins were then transferred onto polyvinylidene difluoride (PVDF) membranes (Merck Millipore, Burlington, USA) via electrotransfer. Membranes were blocked with 5% bovine serum albumin (BSA) in phosphate-buffered saline with Tween-20 (PBST) (Sigma-Aldrich, St. Louis, USA) for one hour to minimize non-specific

binding. Subsequently, membranes were incubated overnight at 4°C with primary antibodies against PCNA at a 1:1000 dilution, followed by incubation with horseradish peroxidase (HRP)-conjugated secondary antibodies. Protein detection was performed using an enhanced chemiluminescence (ECL) reagent (Cytiva, Marlborough, USA), and signals were visualized with the Invitrogen iBright ChemiDoc Imaging System (Thermo Fisher Scientific, Waltham, USA) [38].

a-SMA staining

Tissue sections (5 µm) were deparaffinized in xylene and rehydrated through a series of graded ethanol solutions. Antigen retrieval was performed by heating the sections in citrate buffer (pH 6.0) using a pressure cooker. Endogenous peroxidase activity was quenched by incubating the sections in 3% hydrogen peroxide (H_2O_2) for 10 minutes at room temperature. To minimize non-specific binding, sections were blocked with 5% normal goat serum for one hour at room temperature. Subsequently, sections were incubated overnight at 4°C with a primary antibody against α-SMA at 1:200 (Abcam, Cambridge, UK)). After washing with PBS, sections were treated with a biotinylated secondary antibody (1:200) for one hour at room temperature. Signal amplification was achieved using the avidin-biotin complex (ABC) method, and visualization was performed with diaminobenzidine (DAB) chromogen. Sections were counterstained with hematoxylin, dehydrated, and mounted for microscopic evaluation. α-SMA expression was assessed qualitatively through microscopic examination and quantitatively using ImageJ software (National Institutes of Health, Bethesda, MD, USA), measuring the percentage of the positively stained area and signal intensity.

Collagen staining

Five-micrometer tissue sections were deparaffinized in xylene and rehydrated through a graded ethanol series. Masson's trichrome staining was performed to assess collagen deposition using all reagents from Sigma-Aldrich (Sigma-Aldrich, St. Louis, USA). Tissue sections were initially treated with Bouin's solution at 56°C for 15 minutes to enhance staining contrast. This was followed by incubation in Weigert's iron hematoxylin for five minutes to stain cell nuclei. Cytoplasmic and muscle fiber staining was achieved using Biebrich scarlet-acid fuchsin for five minutes. Collagen fibers were selectively stained by immersing the sections in phosphomolybdic-phosphotungstic acid solution for five minutes, followed by aniline blue for five minutes. To stabilize the staining, sections were treated with 1% acetic acid for two minutes. After completing the staining process, sections were dehydrated through graded ethanol, cleared in xylene, and permanently mounted for microscopic evaluation. Quantitative analysis of collagen deposition was performed using ImageJ FIJI software, measuring the percentage of positively stained areas to evaluate the extent of collagen formation.

Statistical analysis

Shapiro-Wilk test was used to assess data normality. Normally distributed data are presented as mean±SD and analyzed using one-way analysis of variance (ANOVA) with Tukey's honestly significant difference (HSD) for post-hoc comparisons. Non-normally distributed data are presented as median (IQR) and analyzed using the Kruskal-Wallis test, followed by Dunn-Bonferroni post-hoc analysis. Statistical analyses were performed using SPSS version 29.0 (IBM Corp, New York, USA), with $p<0.050$ considered statistically significant.

Results

Effect of MSC-derived secretome on *VEGF* and PCNA expression in third-degree burn wound healing

Effects of MSC-derived secretome on third-degree burn wound healing were evaluated by assessing *VEGF* and PCNA expression in rat skin tissue. PCNA protein expression was analyzed to assess cell proliferation, while *VEGF* gene expression was measured to evaluate angiogenic capacity. MSC-derived secretome significantly increased PCNA and *VEGF* expression in a dose-dependent manner. Burn wounds treated with MSC-derived secretome showed a significant elevation in PCNA protein levels compared to negative control group ($p<0.05$) (**Figure 2A**),

indicating enhanced cell proliferation essential for tissue regeneration. Additionally, MSC-derived secretome significantly upregulated *VEGF* gene expression in the burn wound model compared to negative control group ($p<0.05$) (**Figure 2B**), suggesting that the MSC secretome promoted angiogenesis, improving blood supply and nutrient delivery to the wound site, thereby accelerating healing.

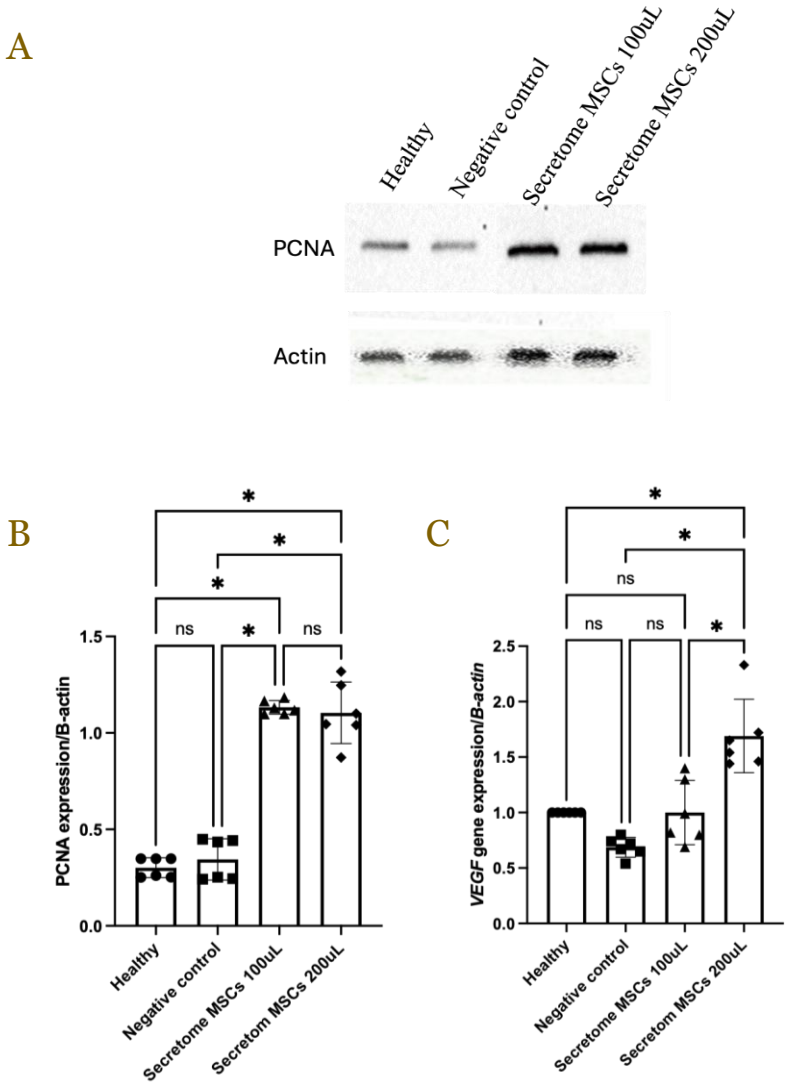

Figure 2. Mesenchymal stem cell-derived secretome treatment increased proliferating cell nuclear antigen (PCNA) protein expression and vascular endothelial growth factor (*VEGF*) gene expression in third-degree burn wound tissues. (A) Western blot analysis of PCNA protein expression in skin samples from a third-degree burn wound model at day 14 post-burn induction. The blot shows bands for PCNA (~29 kDa) and the loading control β-actin (~37 kDa). (B) Quantification of PCNA protein levels from Western blot analysis. (C) *VEGF* gene expression in skin samples. Data are presented as mean ± standard deviation (SD). Statistical analysis used one-way analysis of variance (ANOVA) with Tukey's honestly significant difference (HSD) post-hoc tests. The asterisk (*) indicates statistical significance at $p<0.05$; ns denotes no significant difference.

Effect of MSC-derived secretome on α-SMA expression in third-degree burn wound healing

Treatment with MSC-derived secretome significantly increased α-SMA protein expression, as demonstrated by immunohistochemical staining (**Figure 3A**). Quantitative analysis revealed that the percentage of α-SMA-positive areas increased to 6.12% in the 100 µL MSC-derived secretome-treated group ($p>0.05$) and 12.76% in the 200 µL group ($p<0.05$) compared to the negative control (**Figure 3B**). This increase in α-SMA expression suggested enhanced myofibroblast activity, which plays a crucial role in third-degree burn wound healing.

Dirja et al. Narra J 2025; 5 (2): e1828 - http://doi.org/10.52225/narra.v5i2.1828

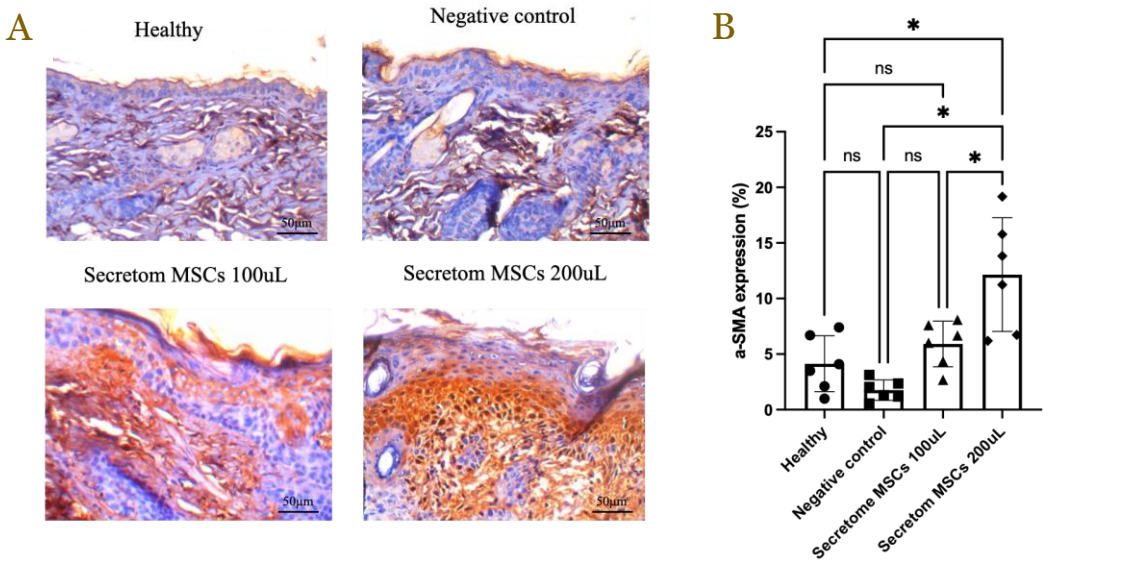

Figure 3. Immunohistochemical (IHC) staining of alpha-smooth muscle actin (α-SMA) at day 14 post-burn induction following mesenchymal stem cell-derived secretome treatment. (A) Representative IHC images of skin tissue sections stained with α-SMA antibody at 100× magnification. (B) Quantification of α-SMA protein expression, presented as the percentage of α-SMA-positive area relative to the total tissue area. Statistical analysis used one-way analysis of variance (ANOVA) with Tukey's honestly significant difference (HSD) post-hoc tests. The asterisk (*) indicates statistical significance at $p<0.05$; ns denotes no significant difference.

Effect of MSC-derived secretome on collagen production in third-degree burn wound healing

Increased collagen density following MSC-derived secretome treatment corresponded with changes in α-SMA expression. Masson's trichrome staining demonstrated a dose-dependent enhancement in collagen deposition in burn wounds treated with MSC-derived secretome (**Figure 4A**). Quantitative analysis indicated a significant increase ($p<0.05$) in collagen levels with higher secretome concentrations, with the 200 µL dose leading to the most pronounced effect, reaching 81.26% ($p<0.05$ compared to all groups) (**Figure 4B**). This enhanced collagen deposition suggested accelerated wound healing and improved tissue structural integrity.

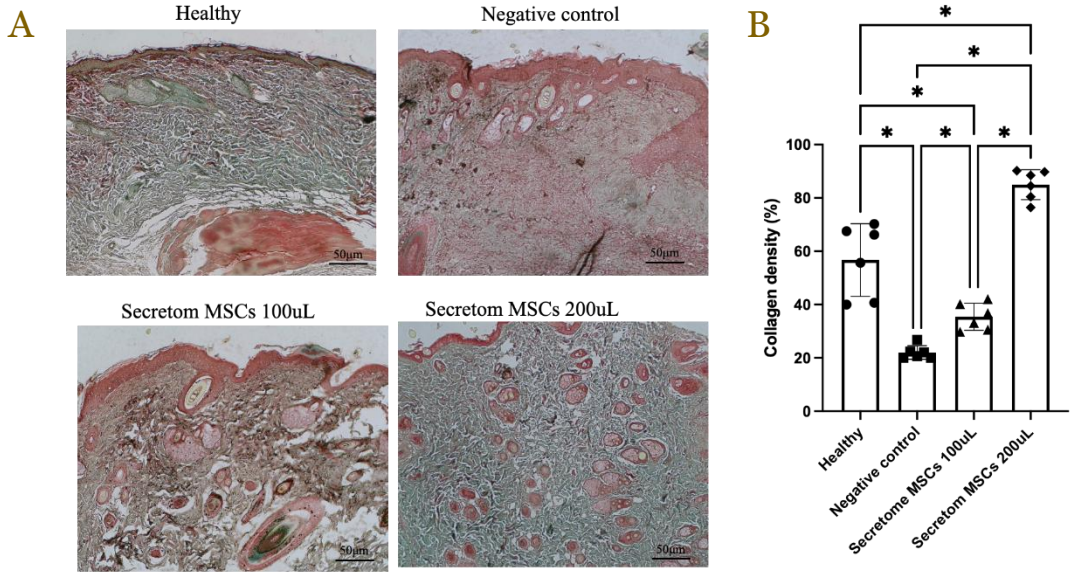

Figure 4. Masson's trichrome staining for collagen at day 14 post-burn induction following mesenchymal stem cell-derived secretome treatment. (A) Representative images of stained skin tissue sections at 100× magnification. (B) Quantification of collagen density, presented as the percentage of the stained area relative to the total tissue area. Statistical analysis used one-way analysis of variance (ANOVA) with Tukey's honestly significant difference (HSD) post-hoc tests. The asterisk (*) indicates statistical significance at $p<0.05$; ns denotes no significant difference.

Discussion

The present study demonstrated the therapeutic potential of MSC-derived secretome in promoting burn wound healing by enhancing the expression of PCNA, *VEGF*, α-SMA, and collagen. These findings confirmed that MSC-derived secretome facilitates burn wound repair through multiple cellular mechanisms, as demonstrated in a rat model. The significant upregulation of PCNA expression in MSC-derived secretome-treated burn wounds highlights the role of these cells in stimulating cell proliferation [39,40]. PCNA is a well-established marker of proliferating cells, and its increased expression indicates enhanced tissue regeneration, which is essential for effective burn wound healing [8]. These findings aligned with previous studies suggesting that MSCs promote cellular proliferation and accelerate tissue repair [11,20]. Additionally, the upregulation of *VEGF* gene expression in MSC-derived secretome-treated wounds suggests that the secretome enhances angiogenesis. *VEGF* is a key regulator of new blood vessel formation and is essential for nutrient and oxygen delivery to the wound site [9,11]. The increased *VEGF* expression indicates improved vascularization, which facilitates efficient tissue repair [41]. As a potent endothelial cell mitogen, *VEGF* plays a crucial role in vascular and lymphatic system development and maintenance [42]. It promotes endothelial cell proliferation, migration, and extracellular matrix degradation while serving as a survival factor [43] In the acute response to burn injury, *VEGF* increases vascular permeability and induces adhesion molecule expression, supporting the recruitment of inflammatory cells necessary for wound healing [44,45].

VEGF levels began to rise one day after burn wound induction, with a significant increase observed on days 3 and 5, followed by a gradual return to baseline levels by days 7 to 14 [46]. In the present study, *VEGF* expression was higher in the group treated with 200 µL of MSC-derived secretome compared to other groups, and it remained elevated relative to the negative control. Previous studies have demonstrated that *VEGF* plays a crucial role in accelerating burn wound healing following MSC administration, with peak expression occurring between days 3 and 6 [9,13]. The findings of the present study suggested that paracrine factors secreted by MSC-derived secretome, including VEGF, TGF-β, and platelet-derived growth factor (PDGF), contribute to the transition from the inflammatory to the proliferative phase. This effect is mediated by an increase in collagen density, which is associated with burn wound closure [47]. However, VEGF also plays a role in scar tissue formation during the remodeling phase [48]. A previous study comparing dorsum and inguinal skin grafting in a rat model reported an increase in vascular density in both groups, further supporting the role of VEGF in neovascularization and tissue regeneration [49].

The administration of MSC-derived secretome in the present study led to a significant increase in α-SMA protein levels, indicating enhanced myofibroblast activation [50,51]. Additionally, the 200 µL concentration not only increased collagen synthesis but also modulated α-SMA expression, suggesting a balanced remodeling process that may reduce excessive fibrosis and scar formation, thereby promoting more effective wound repair. Myofibroblasts play a crucial role in wound contraction and tissue repair; however, excessive activation may contribute to pathological fibrosis and excessive scar formation [52,53]. The increase in α-SMA expression, particularly at higher concentrations of MSC-derived secretome, suggests a regulated remodeling process that facilitates tissue repair while minimizing fibrotic complications. In addition to modulating myofibroblast activity, MSC-derived secretome influenced collagen synthesis in a dose-dependent manner, as demonstrated by Masson's trichrome staining. Collagen is a key structural protein that maintains the mechanical strength and integrity of the repaired tissue [54]. The significant increase in collagen deposition, particularly in wounds treated with 200 µL of MSC-derived secretome, suggested an accelerated healing process with improved structural organization. This enhancement in collagen synthesis, combined with the controlled regulation of α-SMA expression, indicated that MSC-derived secretome contribute to balanced tissue remodeling, promoting effective wound healing while reducing the likelihood of excessive fibrosis and scar formation [55].

The findings of the present study have significant implications for the existing literature and clinical practice in burn wound management. The present study provides additional evidence supporting the therapeutic potential of MSC-derived secretome in accelerating burn

wound healing through multiple mechanisms. MSC-derived secretome offers a multifaceted approach by enhancing cell proliferation, angiogenesis, myofibroblast activation, and collagen deposition, which may lead to more effective and comprehensive treatment strategies for burn injuries. Furthermore, the demonstrated efficacy of secretome-derived products highlights the potential for cell-free therapies in burn wound management. This approach addresses several limitations associated with traditional cell-based therapies, including immune rejection and tumorigenicity risks, while maintaining regenerative benefits. The findings suggest that MSC-derived secretome could serve as a promising alternative to direct cell transplantation, offering a safer and more accessible therapeutic option for improving burn wound healing outcomes.

The present study had several limitations that should be addressed in future research. The observation period was restricted to 14 days, which may not be sufficient to assess the long-term effects of MSC-derived secretome treatment, including its impact on scar maturation and tissue remodeling. Extending the observation period would provide a more comprehensive understanding of the sustained benefits and potential complications associated with MSC-derived secretome therapy. Additionally, the present study did not assess potential adverse effects or immune responses that could arise following MSC-derived secretome administration. Evaluating immunogenicity, inflammatory responses, and possible off-target effects is essential to ensure the safety and clinical applicability of this approach. Moreover, the present study primarily focused on protein expression and histological changes without exploring the underlying cellular and molecular mechanisms by which MSC-derived secretome interact with host tissues. Future studies should incorporate advanced molecular analyses, such as single-cell RNA sequencing or proteomic profiling, to elucidate the signaling pathways and cellular interactions involved in MSC-derived secretome-mediated wound healing. To further validate the therapeutic potential of MSC-derived secretome, long-term studies should be conducted to monitor wound healing progression, scar formation, and extracellular matrix remodeling over an extended period, potentially spanning several months post-treatment.

Conclusion

MSC-derived secretome enhances third-degree burn wound healing through multiple mechanisms, including increased cellular proliferation, promotion of neovascularization, regulation of myofibroblast activity, and extracellular matrix remodeling. The ability of MSC-derived secretome to accelerate wound closure and improve tissue regeneration highlights its potential as a therapeutic strategy for burn management. The observed improvements in healing suggest that MSC-derived secretome may offer clinical benefits by modulating key processes essential for wound repair. By promoting angiogenesis, facilitating collagen deposition, and balancing myofibroblast activation, MSC-derived secretome contribute to both structural integrity and functional recovery of injured tissue. Further studies are necessary to delineate the precise molecular pathways involved in MSC-derived secretome-mediated wound healing. Additionally, long-term investigations should assess the durability of therapeutic effects, potential adverse reactions, and the applicability of MSC-derived secretome therapy across different burn severities and clinical settings.

Ethics approval

Protocol of the present study was reviewed and approved by the Animal Ethics Committee of the Universitas Islam Sultan Agung Semarang, Semarang, Indonesia (Approval number: 40/AEC/Biomedik/2023).

Acknowledgments

The authors would like to express gratitude to the research staff specializing in stem cell and cancer studies in Semarang, Indonesia, for their valuable contributions to this study.

Competing interests

All authors declare that they have no competing interests.

Funding

The present study was supported by a grant from the Ministry of Research, Technology, and Higher Education of the Republic of Indonesia under the Fundamental Research Scheme 2023.

Underlying data

Derived data supporting the findings of this study are available from the corresponding author on request.

Declaration of artificial intelligence use

This study used artificial intelligence (AI) tool and methodology of which AI-based language model ChatGPT was employed in the language refinement (improving grammar, sentence structure, and readability of the manuscript). We confirm that all AI-assisted processes were critically reviewed by the authors to ensure the integrity and reliability of the results. The final decisions and interpretations presented in this article were solely made by the authors.

How to cite

Dirja BT, Putra A, Amalina ND. Mesenchymal stem cell-derived secretome accelerates third-degree burn wound healing: Effects on proliferation, angiogenesis, and fibrosis regulation. Narra J 2025; 5 (2): e1828 - http://doi.org/10.52225/narra.v5i2.1828.

References

1. Jeschke MG, Pinto R, Kraft R, *et al.* Morbidity and survival probability in burn patients in modern burn care. Crit Care Med 2015;43 (4):808-815.
2. Forbinake NA, Ohandza CS, Fai KN, *et al.* Mortality analysis of burns in a developing country: A CAMEROONIAN experience. BMC Public Health 2020;20(1):1269.
3. Jeschke MG, van Baar ME, Choudhry MA, *et al.* Burn injury. Nat Rev Dis Primers 2020;6(1):11.
4. Audrain H, Bray A, De Berker D. Full-thickness skin grafts for lower leg defects: An effective repair option. Dermatol Sur 2015;41(4):493-498.
5. Reddy S, El-Haddawi F, Fancourt M, *et al.* The incidence and risk factors for lower limb skin graft failure. Dermatol Res Pract 2014;2014:51-54.
6. Mohamed ME, Almobarak BA, Hassan MI. Treatment of extensive post-burn deformities using extra-large sheets of full thickness skin grafts. Clin Pract 2017;14(4):249-256.
7. Kwon SH, Barrera JA, Noishiki C, *et al.* Current and emerging topical scar mitigation therapies for craniofacial burn wound healing. Front Physiol 2020;11:916.
8. Kumar S, Maurya VK, Chitti S V., *et al.* Wound healing activity of a novel formulation SKRIN via induction of cell cycle progression and inhibition of PCNA-p21 complex interaction leading to cell survival and proliferation. ACS Pharmacol Transl Sci 2021;4(1):352-364.
9. Wise LM, Stuart GS, Real NC, *et al.* VEGF Receptor-2 Activation Mediated by VEGF-E Limits Scar Tissue Formation Following Cutaneous Injury. Adv Wound Care 2018;7(8):283-297.
10. Khamis T, Abdelalim AF, Saeed AA, *et al.* Breast milk MSCs upregulated β-cells PDX1, Ngn3, and PCNA expression via remodeling ER stress /inflammatory /apoptotic signaling pathways in type 1 diabetic rats. Eur J Pharmacol 2021;905:174188.
11. An Y, Liu WJ, Xue P, *et al.* Autophagy promotes MSC-mediated vascularization in cutaneous wound healing via regulation of VEGF secretion article. Cell Death Dis 2018;9(2):58.
12. Han Y, Tao R, Han Y, *et al.* Microencapsulated VEGF gene-modified umbilical cord mesenchymal stromal cells promote the vascularization of tissue-engineered dermis: An experimental study. Cytotherapy 2014;16(2):160-169.
13. Shams F, Moravvej H, Hosseinzadeh S, *et al.* Overexpression of VEGF in dermal fibroblast cells accelerates the angiogenesis and wound healing function: In vitro and in vivo studies. Sci Rep 2022;12(1):18529.
14. Shi S, Ou X, Long J, *et al.* Nanoparticle-based therapeutics for enhanced burn wound healing: A comprehensive review. Int J Nanomedicine 2024;19:11213-11233.
15. He X, Dong Z, Cao Y, *et al.* MSC-derived exosome promotes M2 polarization and enhances cutaneous wound healing. Stem Cells Int 2019;2019:7132708.

16. Zhao G, Liu F, Liu Z, *et al.* MSC-derived exosomes attenuate cell death through suppressing AIF nucleus translocation and enhance cutaneous wound healing. Stem Cell Res Ther 2020;11(1):1-18.
17. Wu P, Zhang B, Shi H, *et al.* MSC-exosome: A novel cell-free therapy for cutaneous regeneration. Cytotherapy 2018;20(3):291-301.
18. Han Y, Yang J, Fang J, *et al.* The secretion profile of mesenchymal stem cells and potential applications in treating human diseases. Signal Transduct Target Ther 2022;7(1):92.
19. Hamra NF, Putra A, Tjipta A, *et al.* Hypoxia mesenchymal stem cells accelerate wound closure improvement by controlling α-smooth muscle actin expression in the full-thickness animal model. Open Access Maced J Med Sci 2021;9:35-41.
20. Hidayat M, Kusumo B, Husain SA, *et al.* Secretome MSCs restore α-smooth muscle actin protein tissue expression in croton oil-induced hemorrhoid rats. CBS Int J 2023;2(4):139-146.
21. Utami A, Putra A, Wibowo JW, *et al.* Hypoxic secretome mesenchymal stem cells inhibiting interleukin-6 expression prevent oxidative stress in type 1 diabetes mellitus. Med Glas 2023;20(2).
22. Prajoko YW, Putra A, Dirja BT, *et al.* The ameliorating effects of MSCs in controlling treg-mediated B-cell depletion by indoleamine 2, 3-dioxygenase induction in PBMC of SLE patients. Open Access Maced J Med Sci 2022;10:6-11.
23. Nirenjen S, Narayanan J, Tamilanban T, *et al.* Exploring the contribution of pro-inflammatory cytokines to impaired wound healing in diabetes. Front Immunol 2023;14:1216321.
24. Mahmoud NN, Hamad K, Al Shibitini A, *et al.* Investigating Inflammatory Markers in Wound Healing: Understanding Implications and Identifying Artifacts. ACS Pharmacol Transl Sci 2024;7(1):18-27.
25. Hu M, Ludlow D, Alexander JS, *et al.* Improved wound healing of postischemic cutaneous flaps with the use of bone marrow-derived stem cells. Laryngoscope 2014;124(3):642-648.
26. Maranda E, Rodriguez-Menocal L, Badiavas E. Role of mesenchymal stem cells in dermal repair in burns and diabetic wounds. Curr Stem Cell Res Ther 2016;12(1):61-70.
27. Henriksen JL, Sørensen NB, Fink T, *et al.* Systematic review of stem-cell-based therapy of burn wounds: Lessons learned from animal and clinical studies. Cells 2020;9(12):2545.
28. Lunardi LO, Martinelli CR, Lombardi T, *et al.* Modulation of MCP-1, TGF- β 1, and α -SMA expressions in granulation tissue of cutaneous wounds treated with local vitamin B complex: An experimental study. Dermatopathology 2014;1(2):98-107.
29. Penn JW, Grobbelaar AO, Rolfe KJ. The role of the TGF-β family in wound healing, burns and scarring: A review. Int J Burns Trauma 2012;2(1):18-28.
30. Restimulia L, Ilyas S, Munir D, *et al.* The CD4+CD25+FoxP3+ regulatory T cells regulated by MSCs suppress plasma cells in a mouse model of allergic rhinitis. Med Arch 2021;75(4):256-261.
31. Daryanti E, Putra A, Sumarawati T, *et al.* The Comparison of Normoxic and Hypoxic Mesenchymal Stem Cells in Regulating Platelet-derived Growth Factors and Collagen Serial Levels in Skin Excision Animal Models. Open Access Maced J Med Sci 2023;11(A):181-187.
32. Zukhiroh Z, Putra A, Chodidjah C, *et al.* Effect of secretome-hypoxia mesenchymal stem cells on regulating SOD and MMP-1 mRNA expressions in skin hyperpigmentation rats. Open Access Maced J Med Sci 2022;10(A):1-7.
33. Fredianto M, Herman H, Ismiarto YD, *et al.* Secretome of hypoxia-preconditioned mesenchymal stem cells enhance the expression of HIF-1a and bFGF in a rotator cuff tear model. Med Glas 2023;20(2):242-248.
34. Sunarto H, Trisnadi S, Putra A, *et al.* The role of hypoxic mesenchymal stem cells conditioned medium in increasing vascular endothelial growth factors (VEGF) levels and collagen synthesis to accelerate wound healing. Indones J Cancer Chemoprev 2020;11(3):134.
35. Sungkar T, Putra A, Lindarto D, *et al.* Intravenous umbilical cord-derived mesenchymal stem cells transplantation regulates hyaluronic acid and interleukin-10 secretion producing low-grade liver fibrosis in experimental rat. Med Arch 2020;74(3):177-182.
36. Drawina P, Putra A, Nasihun T, *et al.* Increased serial levels of platelet-derived growth factor using hypoxic mesenchymal stem cell-conditioned medium to promote closure acceler- ation in a full-thickness wound. Indones J Biotechnol 2022;27(1):36.
37. Fu X, Fang L, Li X, *et al.* Enhanced wound-healing quality with bone marrow mesenchymal stem cells autografting after skin injury. Wound Repair Regen 2006;14(3):325-335.
38. Jenie RI, Amalina ND, Ilmawati GPN, *et al.* Cell cycle modulation of CHO-K1 cells under genistein treatment correlates with cells senescence, apoptosis and ROS level but in a dose-dependent manner. Adv Pharm Bull 2019;9(3):453-461.

39. Zhu Z, Zhu X, Miao S, *et al.* Mechanism of engineered macrophage membrane bionic gene-carrying nanospheres for targeted drug delivery to promote wound repair in deep second-degree burns. Sci Rep 2025;15(1):2756.
40. Vinaik R, Jeschke MG. Burn-derived mesenchymal stem cells in wound healing. J Dermatol & Skin Sci 2020;2(2):21-26.
41. Putra A, Suwiryo ZH, Muhar AM, *et al.* The Role of Mesenchymal Stem Cells in Regulating PDGF and VEGF during Pancreatic Islet Cells Regeneration in Diabetic Animal Model. Folia Med 2021;63(6):875-883.
42. Almawi WY, Gammoh E, Malalla ZH, *et al.* Analysis of VEGFA variants and changes in VEGF levels underscores the contribution of VEGF to polycystic ovary syndrome. PLoS One 2016;11(11):e0165636.
43. Duffy A, Bouchier-Hayes D, Harmey J. Vascular endothelial growth factor (VEGF) and its role in non-endothelial cells: Autocrine signalling by VEGF. In: Madame Curie Bioscience Database. Austin: Landes Bioscience; 2011.
44. Gianni-Barrera R, Burger M, Wolff T, *et al.* Long-term safety and stability of angiogenesis induced by balanced single-vector co-expression of PDGF-BB and VEGF 164 in skeletal muscle. Sci Rep 2016;6(1):1-15.
45. Fang L, Li Y, Wang S, *et al.* TGF-β1 induces VEGF expression in human granulosa-lutein cells: a potential mechanism for the pathogenesis of ovarian hyperstimulation syndrome. Exp Mol Med 2020;52(3):450-460.
46. Johnson KE, Wilgus TA. Vascular endothelial growth factor and angiogenesis in the regulation of cutaneous wound repair. Adv Wound Care 2014;3(10):647-661.
47. Sunarto H, Trisnadi S, Putra A, *et al.* The role of hypoxic mesenchymal stem cells conditioned medium in increasing vascular endothelial growth factors (VEGF) levels and collagen synthesis to accelerate wound healing. Indones J Cancer Chemoprev 2020;11(3):134.
48. Tang JB, Wu YF, Cao Y, *et al.* Basic FGF or VEGF gene therapy corrects insufficiency in the intrinsic healing capacity of tendons. Sci Rep 2016;6:20643.
49. Zhai Q, Zhou F, Ibrahim MM, *et al.* An immune-competent rat split thickness skin graft model: Useful tools to develop new therapies to improve skin graft survival. Am J Transl Res 2018;10(6):1600-1610.
50. Sousa AM, Liu T, Guevara O, *et al.* Smooth muscle α-actin expression and myofibroblast differentiation by TGFβ are dependent upon MK2. J Cell Biochem 2007;100(6):1581-1592.
51. Gras C, Ratuszny D, Hadamitzky C, *et al.* miR-145 contributes to hypertrophic scarring of the skin by inducing myofibroblast activity. Mol Med 2015;21:296-304.
52. Darby IA, Laverdet B, Bonté F, *et al.* Fibroblasts and myofibroblasts in wound healing. Clin Cosmet Investig Dermatol 2014;7:301-311.
53. Hinz B. Formation and Function of the Myofibroblast during Tissue Repair. J Invest Dermatol 2007;127(3):526-537.
54. Chattopadhyay S, Raines RT. Review collagen-based biomaterials for wound healing. Biopolymers 2014;101(8):821-833.
55. Guillamat-Prats R. The role of MSC in wound healing, scarring and regeneration. Cells 2021;10(7):1729.